

## Small hydrocarbons on metal surfaces: adsorption-induced changes in electronic and geometric structure as seen by X-ray absorption spectroscopy

Christof Wöll

*Lehrstuhl für Physikalische Chemie I, Ruhr-Universität Bochum, D-44780 Bochum, Germany.  
E-mail: woell@pc.ruhr-uni-bochum.de*

Monolayers of several unsaturated and saturated hydrocarbons (ethylene, acetylene, benzene, *n*-hexane, cyclohexane, *n*-octane, *n*-hexatriacontane) adsorbed on a number of different metal surfaces [Cu(111), Au(111), Ru(0001) and Pt(111)] have been investigated by carbon *K*-edge X-ray absorption spectroscopy (XAS). Whereas the corresponding multilayer data qualitatively resemble the core-excitation spectra observed for the free molecules, generally significant modifications are observed in the monolayer data. For the saturated hydrocarbons, a strong quenching of the Rydberg *R* resonance at 287.7 eV and the appearance of a new broad feature at around 285.1 eV (*M* resonance) is observed for molecules in direct contact with the metal surfaces. In the case of the unsaturated hydrocarbons, for a number of metals, distinct new features are seen in the XAS data, revealing significant intramolecular distortions.

**Keywords:** hydrocarbon; metal surface; adsorption; X-ray absorption.

### 1. Introduction

Understanding the fundamentals of molecule–surface interaction is definitely a key issue of basic research. In addition, for many applied fields, *e.g.* adhesion of paints, lubrication and corrosion inhibition, a detailed insight into the properties of a molecular adsorbate is required in order to optimize technical processes or to analyse product failure. If the importance is weighed by the absolute value of the related products, however, heterogeneous catalysis is significantly the most important area where precise information on the interaction of molecules with surfaces is required in order to optimize both total yield and selectivity. As a result of the molecule–adsorbate interaction, the activation barriers for dissociation of the free molecules can be significantly reduced so that even rather unreactive molecules can be transformed without having to go to high temperatures. Today, a particular challenging area is the field of C–H bond activation. Transforming *e.g.* methane, CH<sub>4</sub>, into higher alkanes, is an issue of key importance for the transport of natural gas over long distances.

Considering the advances in theoretical chemistry, it would be desirable to reach a point where these molecule/surface interactions can be analysed on the theoretical grounds, thus largely reducing the immense experimental effort in determining details on the electronic structure for a given adsorbate. Here it is worth pointing out that for a large number of hydrocarbon–metal interactions, such an understanding is just emerging. Recently, the interactions of various unsaturated hydrocarbons, *e.g.* ethylene, acetylene and benzene, with *e.g.* Cu surfaces have been investigated theoretically (Hermann & Witko, 1995; Pettersson *et al.*, 1998) and a consistent picture is beginning to emerge. By comparing such theories with the available experimental data on the electronic structure, however, it has become clear that the information provided by the standard technique used in

this field, UPS (ultraviolet photoelectron spectroscopy) is often not sufficiently detailed to obtain even a qualitative insight into the fundamental phenomena.

A further important detail of adsorbed hydrocarbons, of course, is their geometric arrangement at the surface, where both site geometries and intramolecular changes are of interest. Here significant success has been achieved in determining precise positions of adsorbate atom centres with low-energy electron diffraction (LEED) and, more recently, photoelectron diffraction (PED) measurements. Examples are acetylene adsorbed on Cu(111) (Bao *et al.*, 1993) and Ni(111) (Bao *et al.*, 1994, 1995; Somorjai, 1994), ethylene on Ni(111) (Boa *et al.*, 1995; Somorjai, 1994) and benzene on Ni(111) (Schaff *et al.*, 1996). While LEED and PED techniques yield rather precise positions of carbon and heavier atoms inside adsorbed molecules, they cannot give information about the positions of hydrogen centres because of problems with small scattering cross sections. This is of particular relevance for adsorbed hydrocarbons where intramolecular distortions as a result of adsorption affect both C–C and C–H bond lengths, as well as the respective C–C–H and H–C–H bending angles. Thus, for a more detailed understanding of the role of the H atoms and the nature of the adsorbate complex, it is important to gather information on the exact position of the H atoms. This is confirmed by recent theoretical studies (Hermann & Witko, 1995; Hermann *et al.*, 1996) which have provided strong evidence for rather large intramolecular distortions inside acetylene adsorbed on Cu(111) with the C–H bonds being bent away from the centre C–C axis by as much as 60°. Similar results were obtained for benzene adsorbed on a Cu(110) surface (Pettersson *et al.*, 1998).

In the following, it will be demonstrated that C 1s X-ray absorption spectroscopy can contribute significantly to the understanding of hydrocarbon–metal surface interaction by providing information that is complementary to that obtained with the standard techniques. Although near-edge X-ray absorption fine structure (NEXAFS) is mostly used to obtain information on the molecular orientation at surfaces, it will be demonstrated here that direct information on adsorption-induced intramolecular distortions in adsorbed unsaturated hydrocarbons, as well as adsorption-induced changes in molecular electronic structure for saturated hydrocarbons, can be obtained in a rather straightforward fashion.

To begin with, the case of unsaturated hydrocarbons will be considered, by first examining two rather simple molecules, acetylene and ethylene, adsorbed on Cu(111). It will be demonstrated that the large intramolecular distortion predicted by theory (see above) is corroborated in a rather direct way by NEXAFS. For ethylene adsorbed on the same surface, the theoretical calculations yielded two minima in the energy *versus* distance curve, one corresponding to a strongly distorted di- $\sigma$ -bonded species and the second, at larger distances, corresponding to a physisorbed, undistorted molecule. The NEXAFS data provided direct evidence that exposure to ethylene at room temperature results in the formation of an essentially planar adsorbate. The discussion of the unsaturated hydrocarbons will be concluded by considering the case of benzene adsorbed on a variety of different metals, ranging from the rather unreactive gold to the catalytically active platinum. In this case, the NEXAFS data directly reveal the transition from a physisorbed, essentially planar benzene molecule, adsorbed with its ring plane planar with respect to the Au surface, to a strongly chemisorbed, strongly distorted adsorbate on the Pt surface, where the C–H bonds are bent away from the surface plane by an amount similar to that discussed for acetylene (see above).

Whereas for the interaction of unsaturated hydrocarbons with solid substrates the theoretical understanding has made tremendous

progress, the exact nature of adsorbed saturated hydrocarbons, *e.g.* alkanes, is still far from being understood. On most metal surfaces, these rather unreactive molecules adsorb in an associative fashion and measurements of the binding energies yield values consistent with the presence of a physisorbed species. The force constant coupling the hydrocarbons to the surface has been determined and is also consistent with a weak molecule–surface interaction only (Witte & Wöll, 1995). Since saturated hydrocarbons reveal a large band-gap difference of around 7 eV between LUMO (lowest unoccupied molecular orbital) and HOMO (highest unoccupied molecular orbital), a significant interaction with the metal, *i.e.* donation of charge from molecular states into the metal, back-donation from metal states to the molecule, as *e.g.* in the case of CO adsorbed on a metal surface, is not expected. This belief is in accord with experimental data obtained on the electronic structure using UPS (ultra-violet photoelectron spectroscopy) (Weckesser *et al.*, 1997; Yoshimura *et al.*, 1998), which does not show any anomalies. Briefly, the data are consistent with a superposition of substrate and molecular electronic charge.

There are, nevertheless, several properties of the adsorbed saturated hydrocarbons which are incompatible with the presence of a physisorbed species. The most disturbing observation dates back 25 years, when, using electron energy loss spectroscopy (EELS), Demuth *et al.* (1978) observed a huge softening of the C–H stretch vibration in cyclohexane adsorbed on Ni(111) and Pt(111). Although since then similar observations have been reported for many other systems (Raval & Chesters, 1989; Hostetler *et al.*, 1995; Yamamoto *et al.*, 2000), only few theoretical investigations have been undertaken (Hoffmann & Upton, 1984; Kang & Anderson, 1985) in order to understand the nature of this particular interaction. Another disturbing observation has been made with NEXAFS, where a distinct new resonance,  $M^*$  was observed and related to an interaction between the molecule and the metal surface. By carrying out experiments on a clean and a hydrogen-passivated Ru surface, it could be demonstrated that the presence of the soft C–H modes discussed above and the  $M^*$  resonance are related (Witte *et al.*, 1998).

Data obtained with UPS for monolayers of different alkanes adsorbed on Cu(111) (Weckesser *et al.*, 1997), however, did not provide any new insight, since the high electronic density of states at the metal surfaces, in particular that of the *d* bands, effectively obscures the expected changes. X-ray absorption spectroscopy at the C 1s edge is significantly more sensitive, since, owing to the nature of the excitation process, only those final states for which the contribution from atomic C 2*p* orbitals is finite are seen by this technique. As a consequence, electronic states of pure metal character are suppressed and instead of the total density of states as seen in UPS, the molecule-related partial density of states is detected.

In Fig. 1, this important aspect is illustrated. The LUMO of a complex consisting of a 38-atom Cu cluster, simulating a Cu(111) surface, and the smallest cyclic saturated hydrocarbon, cyclopropane ( $C_3H_6$ ), are shown at the top of Fig. 1 for a molecule–surface distance of 5 Å, and at the bottom for a distance of 7.5 Å. One C atom in the cyclopropane is core-excited. For the large distance, the molecule and the metal cluster are almost completely decoupled electronically, and as a result the LUMO is of pure molecular character. If the distance is decreased, however, electronic interactions become significant and, as a result, a considerable mixing of metal cluster and cyclopropane electronic states is observed (see the top of Fig. 1). The unambiguous proof of the existence of such electronic hybrid states with UPS is difficult, but rather straightforward with NEXAFS. The latter fact is due to the projection of the adsorbate molecular orbitals onto the carbon 2*p* orbitals. If the states have a pure metal character, the states

are invisible in the C 1s NEXAFS spectra. If, on the other hand, features are seen at the energy corresponding to the Fermi edge [approximately the X-ray photoelectron spectroscopy (XPS) C 1s binding energy], one can immediately conclude a hybrid character of the corresponding orbitals.

In the present paper, the results of a systematic investigation on the electronic structures of different alkane monolayers (*n*-hexane, cyclohexane, *n*-octane, *n*-hexatriacontane) adsorbed on Cu, Au, Ru and Pt metal surfaces using NEXAFS spectroscopy are summarized. Clear evidence is found for adsorption-induced electronic structure changes, *i.e.* a quenching of the Rydberg resonances and the creation of a broad resonance at 285.1 eV. The latter apparently correlates with the above-mentioned anomalous soft C–H stretching vibrations. A precise determination of coverages using XPS allows the

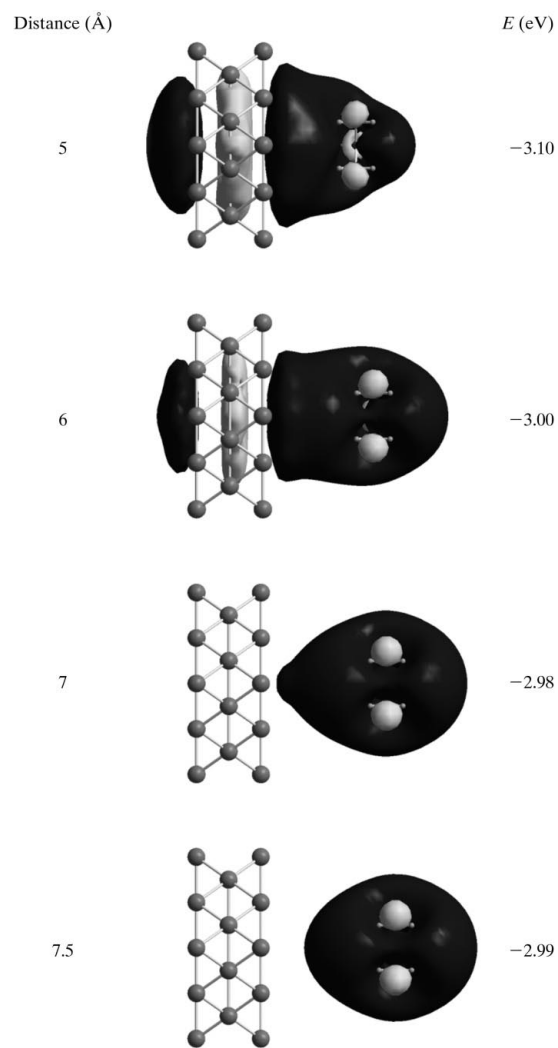


**Figure 1**

The lowest unoccupied molecular orbital (LUMO) of a cyclopropane–Cu(38) complex for different distances. The Cu(38) cluster simulating a Cu(111) surface consisted of three layers with 13 atoms in the top plane, 12 atoms in the centre plane and 13 atoms in the bottom plane. The corresponding *ab initio* Hartree–Fock (HF) calculations were carried out with the GAUSSIAN98 program package using the equivalent cores approximation (ECA) (Weiss *et al.*, 1999). In these HF calculations, an augmented double- $\zeta$  basis set was used for the C and H atoms (Weiss *et al.*, 1999) and a one-electron effective core potential (Laskowski & Bagus, 1984) for the Cu atoms. Whereas for large distances the LUMO is clearly of molecular character only (bottom), for smaller distances the orbital develops a pronounced hybrid character (top).

conclusion to be drawn that only molecules in the first monolayer are involved in the interactions which give rise to these new states.

## 2. Experimental

The experiments were performed at the beamline HE-TGM2 of the synchrotron radiation facility BESSY (Berlin) using a multi-chamber ultra-high vacuum (UHV) system operated in the low  $10^{-10}$  mbar pressure range. The metal substrates were cleaned by standard procedures, including a series of Ar-sputtering and annealing cycles. The cleanliness and quality of the surfaces were checked by XPS and LEED. All smaller molecules used in the experiments (ethylene, acetylene, benzene, cyclohexane, *n*-hexane and *n*-octane) were adsorbed from the gas phase onto cooled metal substrates by back-filling the UHV system through a leak valve connected to a glass container filled with the corresponding high-purity liquids. To remove volatile impurities, a series of freeze-pump-thaw cycles were performed. The long-chain *n*-alkane hexatriacontane ( $C_{36}H_{76}$ ) was supplied by Fluka and deposited from a stainless-steel Knudsen cell. The cell was out-gassed for 1 h at a temperature of 370 K and was subsequently heated to the deposition temperature of 400 K. The average deposition rate was controlled with a quartz-crystal microbalance. Monolayers of this molecule were prepared with a deposition rate of  $2 \text{ \AA min}^{-1}$ .

The NEXAFS spectra were recorded by partial electron yield detection with a channeltron by using a retarding voltage of  $-150 \text{ V}$ . Simultaneously with each NEXAFS spectrum, the photocurrent of a carbon-contaminated gold grid was recorded and used as a photon flux monitor. In addition, photoemission yield spectra of a freshly sputtered clean Au sample were recorded in regular time intervals; these spectra were used to normalize the NEXAFS spectra with regard to the transmission function of the monochromator and the mirrors of the beamline.

For energy calibration, the spectra were referenced to a characteristic peak at  $285.0 \text{ eV}$  in the photocurrent spectra of the carbon-contaminated gold grid. The position of this peak was in turn cali-

brated against the strong  $\pi^*$  resonance of HOPG (highly oriented pyrolytic graphite), at  $285.38 \text{ eV}$  (Batson, 1993).

X-ray absorption spectra of monolayer films with an average thickness below  $10 \text{ \AA}$  contain a strong signal from the substrate. In order to separate the adsorbate signal from the substrate contribution, the following procedure was used. First, the NEXAFS spectra of the adsorbate-covered substrate were normalized to unity at  $280 \text{ eV}$  and subsequently a spectrum of the clean substrate, which was normalized correspondingly, was subtracted. At photon energies of  $280 \text{ eV}$ , the photoelectron yield of the metal substrate dominates the signal of the carbon adsorbate. From multilayer spectra, it is known that the carbon signal at  $280 \text{ eV}$  (resulting from absorption by  $C 2s$  and  $C 2p$  photoelectron emission) amounts to about 5% of the edge jump at  $325 \text{ eV}$ . Neglecting the carbon contribution at the energy of  $280 \text{ eV}$ , this subtraction procedure implicitly corrects for the attenuation of the metal electrons in monolayer and multilayer films. Normalization to the photon flux was obtained by taking the ratio of these spectra and a spectrum recorded for the clean Au ample. Finally, the NEXAFS spectra were normalized to unity at  $325 \text{ eV}$ , at which no angular-dependent structures are expected. Selected samples were also investigated with XPS using monochromated Al  $K\alpha$  radiation of  $h\nu = 1486.6 \text{ eV}$ .

## 3. Results

### 3.1. Acetylene adsorbed on Cu(111)

Fig. 2 shows results from NEXAFS measurements on the  $C_2H_2/Cu(111)$  system for which spectra were recorded for normal ( $\Theta = 90^\circ$ ) and off-normal ( $\Theta = 30^\circ$ ) photon incidence. Here  $\Theta$  denotes the angle between the **E** vector of the (linearly polarized) photons and the surface normal. For comparison, an experimental spectrum of  $C_2H_2$  molecules in the gas phase is also included. The spectrum of the free molecules shows one major absorption peak at  $285.9 \text{ eV}$ , which is assigned to a transition of  $C 1s$  core electrons to the LUMO  $1\pi_g$  orbitals that are twofold degenerate and described by antisymmetric combinations of  $C 2p$  functions. As discussed above, the interaction of  $C_2H_2$  with the  $Cu(111)$  surface distorts the linear geometry of the free molecule and, as a result, lifts the degeneracy of the two  $1\pi_g$  orbitals, giving rise to two absorption resonances, at  $283.9$  and  $285.9 \text{ eV}$  (see Fig. 2). The larger component centred at  $285.9 \text{ eV}$  is strongest at normal photon incidence and optical selection rules governing the  $C 1s \rightarrow$  LUMO excitations can be used to assign this feature to transitions to the  $1\pi_{g(=)}$  derived orbital which extends parallel to the  $Cu(111)$  surface plane. Accordingly, the smaller component at lower photon energies has to be assigned to transitions to the  $1\pi_{g(\perp)}$  derived orbital which extends normal to the surface.

The data of Fig. 2 measured at off-normal ( $\Theta = 30^\circ$ ) photon incidence with linear polarization along the plane perpendicular to the surface show a reduction of the peak contribution from transitions to the  $1\pi_{g(=)}$  derived orbital, while that from transitions to the  $1\pi_{g(\perp)}$  derived orbital remains almost constant. The latter may be taken as a clear indication of the presence of a strong molecular distortion, as pointed out

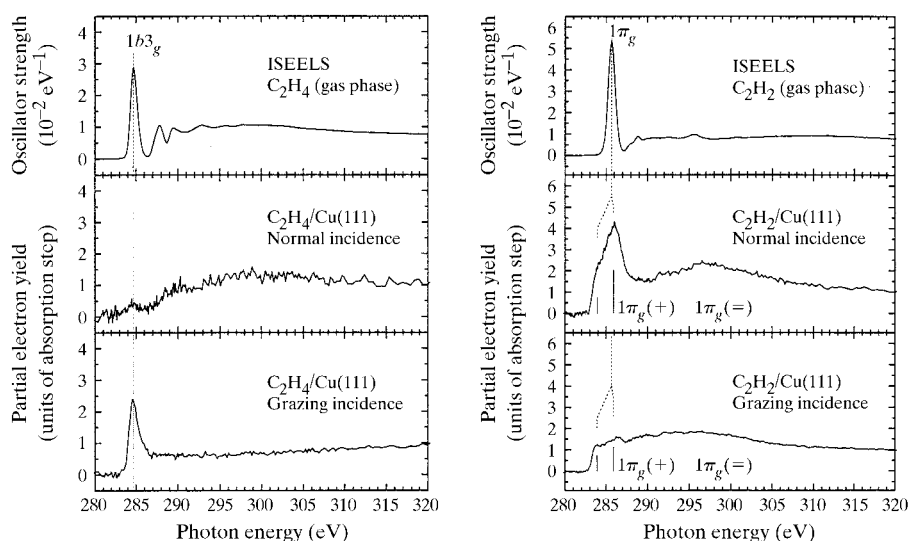


**Figure 2**

Left: NEXAFS spectra recorded at normal incidence (centre) and near grazing incidence (bottom) for monolayers of acetylene adsorbed on  $Cu(111)$  at a temperature of  $100 \text{ K}$ . The corresponding gas-phase data (from Hitchcock & Mancini, 1994) are shown at the top. Right: NEXAFS spectra recorded for an ethylene monolayers adsorbed on  $Cu(111)$  at normal (center) and near grazing (bottom) incidence. The corresponding gas-phase data (from Hitchcock & Mancini, 1994) are shown at the top.

previously (Mainka *et al.*, 1995) and consistent with the bending of the CH ends in adsorbed  $C_2H_2$ . This has been confirmed by simple model studies on the isolated  $C_2H_4$  molecule (Fuhrmann *et al.*, 1998).

### 3.2. Ethylene chemisorbed on Cu(111)

The NEXAFS results on the  $C_2H_4/Cu(111)$  system are shown in Fig. 2 for normal ( $\Theta = 90^\circ$ ) and off-normal ( $\Theta = 30^\circ$ ) photon incidence. Here, the energetically lowest core hole excitation in the free planar molecule corresponds to a transition  $C\ 1s \rightarrow 1b_{3g}$ , where the LUMO  $1b_{3g}$  is represented by an antisymmetric combination of  $C\ 2p$  functions resembling the  $1\pi_{g(L)}$  LUMO of  $C_2H_2$ . Thus, assuming an unperturbed planar molecule at the surface and normal photon incidence, the  $C\ 1s \rightarrow$  LUMO transition should not be excited as a result of optical selection rules. This is consistent with the NEXAFS data for normal incidence shown in Fig. 2, where only a very tiny peak is identified at 285 eV. In contrast, the NEXAFS data for off-normal ( $\Theta = 30^\circ$ ) photon incidence with linear polarization along the plane perpendicular to the surface show a sizeable peak at 285 eV, which obviously arises from the  $C\ 1s \rightarrow 1b_{3g}$  transition, again consistent with the presence of an unperturbed planar  $C_2H_4$  molecule oriented parallel to the Cu(111) surface. Thus, the NEXAFS experiments seem to exclude a strongly distorted  $C_2H_4$  adsorbate as found for the inner potential minimum in the theoretical calculations. In order to test this result,  $C\ 1s$  to LUMO excitations of the  $C_2H_4$  molecule were calculated using *ab initio* Hartree–Fock (HF) wavefunctions, completely analogous to the procedure described above for  $C_2H_2$  (Fuhrmann *et al.*, 1998). The results from the model calculations distinguish clearly between the planar free molecule geometry and that of a distorted  $C_2H_4$  adsorbate. Obviously, the variation of the transition probability of the  $C\ 1s$  to LUMO excitations with photon incidence angle  $\Theta$  is much more pronounced for the planar than for the distorted  $C_2H_4$  molecule. Thus, the theoretical model data confirm the experimental finding of a weakly perturbed physisorbed  $C_2H_4$  species on Cu(111), consistent with data available from He-atom scattering (Fuhrmann *et al.*, 1998). Note that on the more open Cu(110) surface, the presence of a different, more strongly adsorbed ethylene species has been found (Triguero *et al.*, 1998). These differences are attributed to the higher reactivity of the Cu(110) surface.

### 3.3. Benzene adsorbed on a series of different metal surfaces: Au(111), Cu(111), Pt(111) and Rh(111)

A NEXAFS spectrum recorded at the  $C\ 1s$  edge for a thick benzene multilayer is shown at the top of Fig. 3. The spectrum, which is very similar to the gas-phase spectrum of benzene observed by Horsley *et al.* (1985) in an early ISEELS (inner shell electron energy loss spectroscopy) study, is dominated by a strong  $\pi^*$  resonance at 285.2 eV (labelled resonance 1), which can be assigned to an excitation into the lowest unoccupied  $e_{2u}$  orbital of benzene. For an assignment of the other resonances see the work by Weiss *et al.* (1998). The lower part of Fig. 3 contains polarization-dependent NEXAFS spectra of benzene monolayers adsorbed on Au(111), Rh(111) and Pt(111), recorded at normal and grazing photon incidence under the same experimental conditions. For the Au(111) surface, the benzene NEXAFS spectra show a strong angular dependence, which reveals a high degree of molecular orientation. The  $\pi^*$  resonance located at 285.1 eV is very intense at grazing photon incidence and practically absent at normal incidence.

The spectra of strongly chemisorbed benzene monolayers on Rh(111) and Pt(111) are similar to spectra reported earlier for benzene chemisorbed on Pt(111) (Triguero *et al.*, 1998) and several other metal surfaces, *e.g.* Mo(110) (Liu & Friend, 1988; Liu *et al.*,

1990). In contrast to the spectra of physisorbed benzene on Au(111), several pronounced differences can be observed between the monolayer and multilayer spectra. The most conspicuous features are the broadening of the  $\pi^*$  resonance and the reduction in the linear dichroism. Obviously, the differences with respect to the multilayer spectrum are stronger for Pt than for Rh. The splitting of the  $\pi^*$  resonance is attributed to a hybridization of the  $\pi^*$  orbitals with metal electronic states, leading to the formation of several different hybrid electronic states. The hybrid character of these electronic states enhances the coupling of the final  $\pi^*$  orbital to empty states in the metal conduction band, as pointed out earlier by Stöhr (1992). This leads to a strong decrease of the final state lifetime and thus explains the significant increase in line width when going from the multilayer to the monolayer spectra.

The variation of the  $\pi^*$  resonance intensity with photon angle of incidence only qualitatively resembles the expected polarization dependence for flat lying benzene. For benzene molecules oriented parallel to the substrate, the  $\pi^*$  resonance should be strictly zero at normal incidence, even when considering an X-ray degree of polarization below 100% (Mainka *et al.*, 1995). In the experimental data, however, considerable intensities can be observed for both surfaces, Rh and Pt. The intensity ratio of the  $\pi^*$  resonance at normal incidence with respect to grazing incidence amounts to 0.1 for Rh and to 0.3 for Pt. A naive interpretation of these intensity ratios  $I(90^\circ)/I(30^\circ)$  would yield average tilt angles of  $20^\circ$  on the Rh(111) surface and  $30^\circ$  on the Pt(111) surface, apparently inconsistent with the presence of flat-lying benzene molecules on metal surfaces with high structural quality. Previously, applications of different techniques, including LEED, ARUPS (angle-resolved ultraviolet photoelectron spectroscopy) and high-resolution electron energy loss spectroscopy

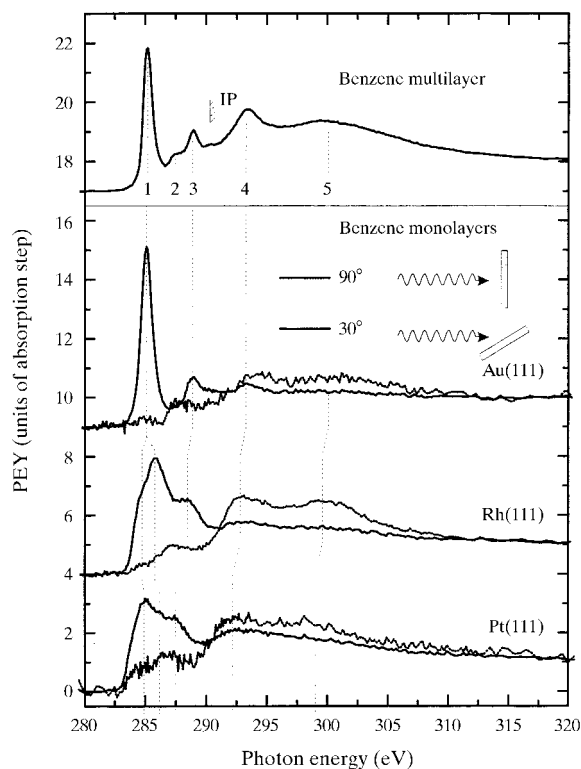


**Figure 3** NEXAFS spectrum of a benzene multilayer at 120 K (top). Polarization dependence of NEXAFS spectra recorded for benzene monolayers adsorbed on Au(111), Rh(111) and Pt(111) (lower part). The spectra were recorded for normal ( $90^\circ$ ) and grazing ( $30^\circ$ ) photon incidence.

(HREELS), have shown that benzene lies flat on Rh(111) (Hove *et al.*, 1983), Pt(111) (Wander *et al.*, 1991) and on a variety of other low-index transition-metal surfaces, and in particular on Ru(0001) (Jakob & Menzel, 1988). It can therefore definitely be excluded that the observed residual intensity is caused by a non-zero tilt angle on these surfaces. In previous work, it has been suggested that the non-zero intensity at normal incidence could be caused by tilted benzene molecules adsorbed at substrate defects like steps (Liu *et al.*, 1990). In order to explain the observed intensity ratios  $I(90^\circ)/I(30^\circ)$ , 5% or 14% of the benzene molecules would have to be adsorbed with their molecular planes perpendicular to the surface plane on Rh(111) or Pt(111), respectively (Mainka *et al.*, 1997).

The concentration of substrate defects was determined independently by thermal desorption experiments with CO and was found to be lower than 1% on the Pt(111) single crystal (Mainka *et al.*, 1997). The concentration of defects is thus too low to explain the residual intensity of the  $\pi^*$  resonance in the case of Pt(111); furthermore, for the other substrates the structural quality of the surfaces allows significant contributions from step edges to be excluded. Accordingly, the unexpectedly weak  $\pi^*$  dichroism has to be attributed to adsorption-induced distortions (bending of the CH bonds away from the metal surface) accompanied by a strong electronic rehybridization. For a detailed discussion of the implications of such a distortion on the NEXAFS spectra see the work by Mainka *et al.* (1995).

Briefly, *ab initio* electronic structure calculations for free benzene reveal that for a hydrogen out-of-plane bend of  $20^\circ$ , an intensity ratio  $I(90^\circ)/I(30^\circ)$  of about 0.1 can be expected (Mainka *et al.*, 1995). Consequently, a CH bend angle of  $20^\circ$  is assigned to benzene adsorbed on Rh(111). This result is fully consistent with the prediction of an earlier theoretical study carried out for this system by Garfunkel *et al.* (1986). The experimental ratio  $I(90^\circ)/I(30^\circ)$  amounts to 0.3 for the Pt(111) surface and indicates a stronger CH upward bend for  $C_6H_6/Pt(111)$  than for  $C_6H_6/Rh(111)$  and was estimated to be larger than  $30^\circ$  (Mainka *et al.*, 1995).

This explanation suggests a direct correlation between the strength of chemisorption and the observed CH bend angles, which is in accord with the binding energies as determined by temperature-programmed desorption (TPD) spectroscopy carried out for various metal surfaces. On Au(111), where the NEXAFS spectra indicate the absence of a non-planar benzene distortion, the desorption temperature amounts to less than 170 K, but is significantly higher for Pt (370–490 K; Tsai & Muettterties, 1982) and Rh (395 K; Koel *et al.*, 1986) surfaces.

### 3.4. Saturated hydrocarbons

In Fig. 4 the experimental C 1s NEXAFS spectra obtained for multilayers of cyclohexane, *n*-hexane, *n*-octane and *n*-hexatriacontane are shown, which were recorded for the X-ray photons incident at an angle of  $55^\circ$ . The spectra are dominated by three resonances, characteristic for saturated hydrocarbons. The dominating Rydberg resonance *R* is located at 287.7 eV for the long-chain alkane *n*-hexatriacontane and at 288.0 eV for the smaller alkanes. This resonance is actually split into several components (Ohta *et al.*, 1990; Bagus *et al.*, 1996) which cannot be resolved with the instrumental resolution of the toroidal grating monochromator ( $\Delta E > 0.6$  eV at the C 1s edge). The further features at around 293.1 eV ( $CC_{\sigma^*}$  resonance) and 301.0 eV ( $CC'$  resonance) are associated with transitions into valence orbitals of the C–C–C backbone, which are split by bond–bond interaction effects (Stöhr, 1992). The NEXAFS spectra of these multilayers are very similar to core-excitation spectra recorded for free hydrocarbons in the gas phase [ISEELS spectra

were taken from the COREX database provided by Hitchcock & Mancini (1994)].

Fig. 5 shows NEXAFS spectra of cyclohexane, *n*-octane and *n*-hexatriacontane for single saturated monolayers physisorbed on Cu(111), which were recorded at normal and grazing photon incidence, where the angle between the electric field vector and the surface normal amounted to 90 and  $30^\circ$ , respectively. These spectra reveal several pronounced differences from the multilayer data. In all cases, the prominent *R* resonance at 287.7 eV is strongly quenched and three new features are observed: one broad resonance centred at 285.1 eV, one sharp peak at 286.9 eV and a broader, somewhat weaker peak at 288.9 eV.

Let us first focus on the spectra recorded for the monolayer of *n*-hexatriacontane (HTC). The  $CC_{\sigma^*}$  resonance at 293.1 eV is strongest for normal incidence. Since the transition dipole moment of this resonance is oriented along the alkane chain (Hähner *et al.*, 1991), this finding is qualitatively in agreement with a flat orientation generally observed for linear alkanes adsorbed on Cu(111) (Weckesser *et al.*, 1997). In the pre-edge region, the NEXAFS spectra reveal strong differences from those recorded for the alkane multilayers. Instead of the prominent *R* resonance at 287.7 eV, three new features can be observed: a broad feature centred at 285.1 eV, labelled  $M^*$ , and two sharp features located at 286.9 eV (resonance  $R'$ ) and at 288.9 eV (resonance  $R''$ ).

Fig. 6 shows polarization-dependent NEXAFS spectra for *n*-octane and *n*-hexane adsorbed on Au(111), Cu(111), Ru(0001) and Pt(111), respectively. These spectra qualitatively resemble those recorded for HTC on Cu(111) in that they also show a broad  $M^*$  resonance

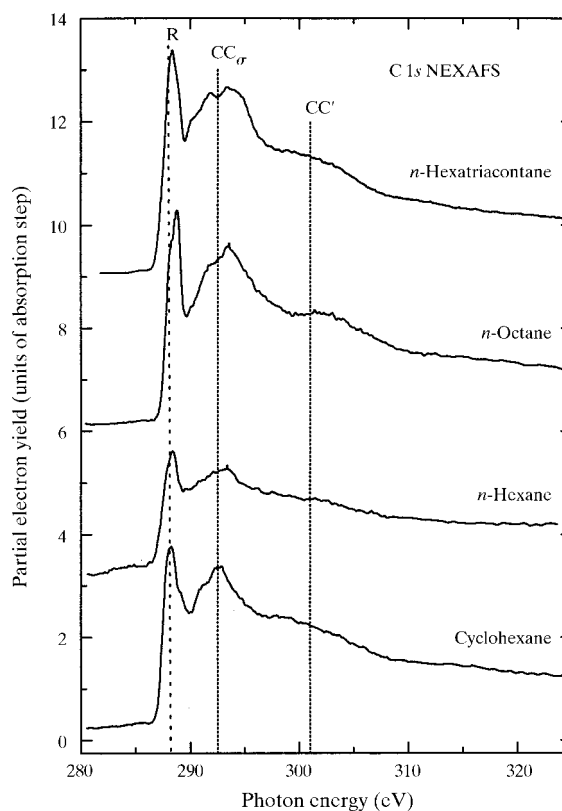


**Figure 4** Multilayer NEXAFS spectra of *n*-hexatriacontane, *n*-octane, *n*-hexane and cyclohexane adsorbed on Cu(111). The spectra were recorded at  $55^\circ$  (angle between the surface normal and the electric field vector of the synchrotron radiation).

centred at 285.1 eV and two sharp features located at around 286.9 eV ( $R'$ ) and 288.9 eV ( $R''$ ), respectively.

In order to aid the assignment of the new resonances, measurements were also carried out for octane adsorbed on a chemically modified Ru(0001) surface. Prior to adsorption of the octane, the surface was hydrogen-saturated by exposure to 1000 L of  $H_2$ . This procedure is known to result in the formation of a well defined  $H(1 \times 1)$  overlayer (Witte *et al.*, 1998). The NEXAFS spectra shown in Fig. 6 (bottom) reveal that the  $M^*$  resonance at 285.1 eV has almost disappeared, while the  $R'$  and  $R''$  resonances are still visible at about the same energies, but are significantly weaker.

Because of the possibility of weak chemical interactions between molecule and substrate, however, it is not immediately obvious whether the new features ( $M^*$ ,  $R'$  and  $R''$ ) have to be assigned to new metal-molecule hybrid orbitals or to Rydberg states shifted by the presence of the polarizable metal substrate.

Let us now consider the feature labelled  $M^*$  at 285.1 eV. This resonance is located just above the threshold for excitations into empty states of metal character. The energy of this threshold is given by the XPS binding energy of the C 1s orbital referenced to the Fermi edge of the metal (Stöhr, 1992), which amounts to 284.2 eV for  $C_{36}H_{76}/Cu(111)$ . The width of this state ( $>2.0$  eV) strongly exceeds the experimental resolution of 0.6 eV. These two observations resemble those reported in NEXAFS studies of benzene adsorbed on a variety of transition-metal surfaces (Mainka *et al.*, 1995; Weiss *et al.*, 1998), where a similar feature just above the threshold energy has been assigned to transitions into orbitals of mixed metal substrate-molecule character. For the present case of alkanes adsorbed on a metal surface, a similar explanation is supported by the observation that the  $M^*$  state is strongly reduced in intensity when octane is

adsorbed on a hydrogen-passivated Ru surface. Thus the  $M^*$  state can be assigned to a superposition of transitions into unoccupied electronic states which are formed upon adsorption of the alkane molecule by a hybridization between molecular and substrate electronic states. This assignment to hybrid orbitals is consistent with a recent multi-technique analysis, in which the occurrence of the  $M^*$  resonance could be shown to correlate with the observation of so-called soft bands in infrared spectroscopy of adsorbed alkanes (see §1) and an unexpected strong damping of the frustrated translation of the molecule normal to the surface (Witte *et al.*, 1998).

In contrast, the new resonances at 286.9 eV ( $R'$ ) and 288.9 eV ( $R''$ ), which are seen best in the grazing-incidence spectrum recorded for hexatriacontane on Cu(111) (see Fig. 5), reveal a smaller half-width. For the sharper  $R'$  peak, a width of 0.6 eV is observed, which essentially corresponds to the experimental resolution. At first sight, it seems that the feature located at 286.9 eV is actually sharper than the  $R$  resonance at 288.7 eV observed for the corresponding multi-layer data (Fig. 4). High-resolution experiments, however, have shown that the  $R$  resonance feature actually consists of three closely spaced, separate resonances corresponding to transitions into three different final states (Bagus *et al.*, 1996). This fine structure could not be resolved with the present monochromator, which has been optimized for the high flux necessary to record spectra of molecules in the monolayer regime.

The small width of the  $R'$  resonance effectively rules out a strong admixing of electronic contributions from metal electronic states. In addition, the data shown in Fig. 6 reveal that the positions of the  $R'$  and  $R''$  resonances are only slightly affected by the hydrogen passivation of the surface. We thus assign the  $R'$  and  $R''$  resonances to final states of molecular character. Since no valence states are expected in

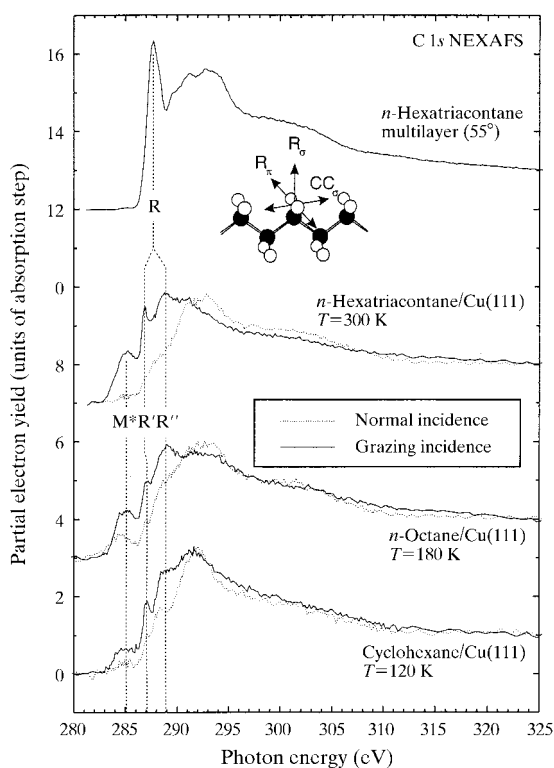


**Figure 5**  
NEXAFS spectra of single saturated monolayers of cyclohexane, *n*-octane and *n*-hexatriacontane adsorbed on Cu(111), recorded at normal ( $90^\circ$ ) and grazing ( $30^\circ$ ) incidence. The spectra are compared to the NEXAFS spectrum of a thick hexatriacontane film (top).

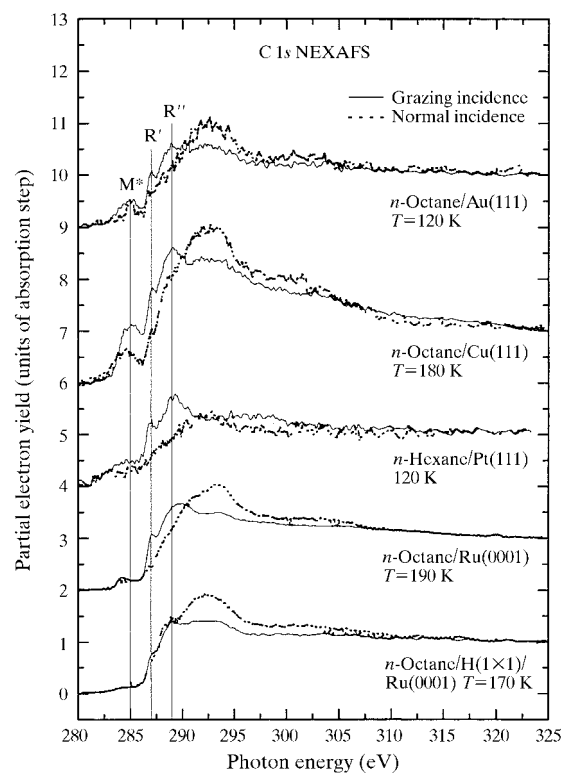


**Figure 6**  
NEXAFS spectra of *n*-octane/Au(111), *n*-octane/Cu(111), *n*-hexane/Pt(111), *n*-octane/Ru(0001) and *n*-octane adsorbed on an H-terminated Ru(0001) surface. All spectra were recorded at normal ( $90^\circ$ ) and grazing ( $30^\circ$ ) incidence.

this energy regime, the most likely assignment is that to molecular Rydberg states. Again, the fact that the  $R'$  (and to a lesser extent the  $R''$  peak) resonance is strongest at grazing incidence, reveals a dominating contribution from  $C\ 2p_z$  orbitals (see above).

Obviously, for a precise assignment, electronic structure calculations for saturated hydrocarbons interacting with a metal substrate similar to those carried out by Bagus *et al.* for the free molecule (Bagus *et al.*, 1996) are required. Unfortunately, such a theoretical analysis represents a formidable task because of the huge basis set required for accurately describing the molecular Rydberg states and, of course, the states of the surface metal atoms. As a result, no recent theoretical studies have been devoted to alkanes adsorbed on metal surfaces, whereas unsaturated hydrocarbons have been the subject of a number of recent studies (Pettersson *et al.*, 1998; Fuhrmann *et al.*, 1998).

#### 4. Conclusions

The examples discussed above demonstrate that carbon  $K$ -edge X-ray absorption spectroscopy is a powerful method for characterizing hydrocarbons adsorbed on metal surface. Since the technique is sensitive to both the electronic and, *via* the linear dichroism, the geometric structure, significant insight could be gained into a number of systems. Whereas for the unsaturated hydrocarbons significant intramolecular distortions have been seen in a number of cases, for saturated hydrocarbons a new feature could be identified, which appears to be the first feature in the electronic structure correlating with the well known soft vibrational modes seen for alkanes on a number of metal surfaces.

Recent experiments have demonstrated that NEXAFS can also be applied in a straightforward fashion to nonmetallic substrates. Since only the number of secondary electrons is detected, a small charging of the substrate does not significantly affect the experimental data. Recently, interesting information has been obtained on the interaction between styrene and different iron oxide surfaces ( $FeO$ ,  $Fe_2O_3$ ) (Wühn *et al.*, 2000; Joseph *et al.*, 2000).

The author gratefully acknowledges collaboration with K. Weiss and many fruitful discussions with P. S. Bagus. This work was in part funded by the German BMBF (contract 05625 VHA3) and the Forschungsmministerium of the State of Nordrhein-Westfalen.

#### References

Bagus, P. S., Weiss, K., Schertel, A., Wöll, C., Braun, W., Hellwig, C. & Jung, C. (1996). *Chem. Phys. Lett.* **248**, 129–135.  
 Bao, S., Hofmann, P., Schindler, K. M., Fritzsche, V., Bradshaw, A. M., Woodruff, D. P., Casado, C. & Asensio, M. C. (1994). *Surf. Sci.* **309**, 722–727.  
 Bao, S., Hofmann, P., Schindler, K. M., Fritzsche, V., Bradshaw, A. M., Woodruff, D. P., Casado, C. & Asensio, M. C. (1995). *Surf. Sci.* **323**, 19–29.  
 Bao, S., Schindler, K. M., Hofmann, P., Fritzsche, V., Bradshaw, A. M. & Woodruff, D. P. (1993). *Surf. Sci.* **291**, 295–308.  
 Batson, P. E. (1993). *Phys. Rev. B*, **48**, 2608–2610.

Delmon, B. & Yates, J. T. (1989). *Surface Science and Catalysis*, Vol. 45. Amsterdam: Elsevier.  
 Demuth, J. E., Ibach, H. & Lehwald, S. (1978). *Phys. Rev. Lett.* **40**, 1044.  
 Fuhrmann, D., Wacker, D., Weiss, K., Hermann, K., Witko, M. & Wöll, C. (1998). *J. Chem. Phys.* **108**, 2651–2658.  
 Garfunkel, E. L., Minot, C., Gavezotti, A. & Simonetta, M. (1986). *Surf. Sci.* **176**, 177.  
 Hähner, G., Kinzler, M., Wöll, C., Grunze, M., Scheller, M. K. & Cederbaum, L. S. (1991). *Phys. Rev. Lett.* **67**, 851.  
 Hermann, K. & Witko, M. (1995). *Surf. Sci.* **337**, 205.  
 Hermann, K., Witko, M. & Michalak, A. (1996). *Z. Phys. Chem.* **197**, 219.  
 Hitchcock, A. P. & Mancini, D. C. (1994). *J. Electron. Spectrosc. Relat. Phenom.* **67**, 1–132.  
 Hoffmann, F. M. & Upton, T. H. (1984). *J. Phys. Chem.* **88**, 6209.  
 Horsley, J. A., Stöhr, J., Hitchcock, A. P., Newbury, D. C., Johnson, A. L. & Sette, F. (1985). *J. Chem. Phys.* **83**, 6099–6107.  
 Hostetler, M. J., Manner, W. L., Nuzzo, R. G. & Girolami, G. S. (1995). *J. Phys. Chem.* **9**, 15269–15278.  
 Hove, M. A. V., Lin, R. F. & Somorjai, G. A. (1983). *Phys. Rev. Lett.* **51**, 778.  
 Jakob, P. & Menzel, D. (1988). *Surf. Sci.* **201**, 503.  
 Joseph, Y., Wühn, M., Niklewski, A., Ranke, W., Weiss, W., Wöll, C. & Schlögl, R. (2000). *Phys. Chem. Chem. Phys.* **2**, 5314–5319.  
 Kang, D. B. & Anderson, A. B. (1985). *J. Am. Chem. Soc.* **107**, 7858.  
 Koel, B. E., Crowell, J. E., Mate, C. M. & Somorjai, G. A. (1986). *J. Phys. Chem.* **90**, 2949.  
 Laskowski, B. C. & Bagus, P. S. (1984). *Surf. Sci.* **138**, 1142.  
 Liu, A. C. & Friend, C. M. (1988). *J. Chem. Phys.* **89**, 4396.  
 Liu, A. C., Stöhr, J., Friend, C. M. & Madix, R. J. (1990). *Surf. Sci.* **235**, 107.  
 Mainka, C., Bagus, P. S., Schertel, A., Strunskus, T., Grunze, M. & Wöll, C. (1995). *Surf. Sci.* **341**, L1055.  
 Mainka, C., Wegner, H., Schertel, A., Wöll, C. & Grunze, M. (1997). *Z. Phys. Chem.* **198**, 221–243.  
 Ohta, T., Seki, K., Yokoyama, T., Morisada, I. & Edamatsu, K. (1990). *Phys. Scr.* **41**, 150.  
 Petterson, L. G. M., Agren, H., Luo, Y. & Triguero, L. (1998). *Surf. Sci.* **408**, 1–20.  
 Raval, R. & Chesters, M. A. (1989). *Surf. Sci.* **219**, L505.  
 Schaff, O., Fernandez, V., Hofmann, P., Schindler, K.-M., Theobald, A., Fritzsche, V., Bradshaw, A. M., Davis, R. & Woodruff, D. P. (1996). *Surf. Sci.* **348**, 89–99.  
 Somorjai, G. A. (1994). *Introduction to Surface Chemistry and Catalysis*. New York: John Wiley.  
 Stöhr, J. (1992). *NEXAFS Spectroscopy*. Berlin: Springer.  
 Triguero, L., Petterson, L. G. M., Minaev, B. & Agren, H. (1998). *J. Chem. Phys.* **108**, 1193–1205.  
 Tsai, M. C. & Muetterties, E. L. (1982). *J. Am. Chem. Soc.* **104**, 2534.  
 Wander, A., Held, G., Hwang, R. Q., Blackman, G. S., Xu, M. L., de Andres, P., Hove, M. A. V. & Somorjai, G. A. (1991). *Surf. Sci.* **249**, 21.  
 Weiss, K., Bagus, P. S. & Wöll, C. (1999). *J. Chem. Phys.* **111**, 6834.  
 Weiss, K., Gebert, S., Wühn, M., Wadepohl, H. & Wöll, C. (1998). *J. Vac. Sci. Technol. A*, **16**, 1017–1022.  
 Weckesser, J., Fuhrmann, D., Weiss, K., Wöll, C. & Richardson, N. V. (1997). *Surf. Rev. Lett.* **4**, 209–218.  
 Witte, G., Weiss, K., Jakob, P., Braun, J., Kostov, K. L. & Wöll, C. (1998). *Phys. Rev. Lett.* **80**, 121–124.  
 Witte, G. & Wöll, C. (1995). *J. Chem. Phys.* **103**, 5860–5863.  
 Wühn, M., Joseph, Y., Bagus, P. S., Niklewski, A., Püttner, R., Reiß, S., Weiss, W., Martins, M., Kaindl, G. & Wöll, C. (2000). *J. Phys. Chem. B*, **104**, 7694–7701.  
 Yamamoto, M., Sakurai, Y., Hosoi, Y., Ishii, H., Kajikawa, K., Ouchi, Y. & Seki, K. (2000). *J. Phys. Chem. B*, **104**, 7370–7376.  
 Yoshimura, D., Ishii, H., Ouchi, Y., Ito, E., Miyamae, T., Hasegawa, S., Ueno, N. & Seki, K. (1998). *J. Electron. Spectrosc. Relat. Phenom.* **88**, 875–879.